

Drilling rotation constraint for shell elements in implicit and explicit analyses

Tobias Erhart¹, Thomas Borrvall²

¹Dynamore GmbH, Stuttgart, Germany

²Dynamore Nordic AB, Linköping, Sweden

Summary:

A subordinate but interesting detail in theory and application of shell elements is investigated in this study, namely the drilling rotation constraint approach. Standard shell elements exhibit 3 translational and 3 rotational degrees-of-freedom at each node. While two nodal rotations are directly associated with bending and twisting modes, the third rotation about the shell normal (also known as the drilling rotation) does not provide any resisting force or stiffness by itself. This fact leads to zero valued components in the stiffness matrix for implicit analyses, which in turn results in a system of equations that cannot be solved. Therefore a small amount of stiffness in form of a torsional spring is artificially added just to remedy the singularity but not to affect the solution too much. This is absolutely necessary to deal with implicit analysis, otherwise no results could be obtained. On the other hand, it might be helpful to have this option also available in explicit analyses to improve results in special situations. It is the intention of this paper to present the theoretical background of this phenomenon and to illustrate the influence of the constraint method in several numerical examples.

Keywords:

Shell elements, Drilling degree-of-freedom, Constraint method

1 Introduction

The standard LS-DYNA shell elements, e.g. the under integrated Belytschko-Lin-Tsay shell (element type 2) or the fully integrated shell with assumed strain interpolation (element type 16), do not possess stiffness in the normal rotational degree of freedom. On the one hand, this drilling degree of freedom is automatically constrained for curved shell topologies, since there the drill rotation automatically creates bending in neighbouring elements. On the other hand, flat shell topologies allow unconstrained rotation of this drilling degree of freedom, i.e. a singular mode is obtained. In implicit analyses, this would lead to a singular stiffness matrix, therefore some constraint must be added. To accomplish that in the implicit solver of LS-DYNA, a consistent drilling constraint approach is used by default, where the stiffness matrix is modified such that the singularity is abolished. This feature can be adjusted via parameters DRCM (method) and DRCPRM (scaling factor) on *CONTROL_IMPLICIT_SOLVER [1].

In explicit analyses, this unconstrained drilling degree of freedom usually does not create any difficulties, because no stiffness matrix is needed. Therefore, no counter measure is necessary by default. Nonetheless, special situations might occur, where an additional resisting rotational force might be helpful to increase robustness and/or accuracy. Beginning with LS-DYNA release R7.0.0, it is possible to activate the consistent drilling constraint for explicit simulations too. This is done via new parameters DRCPSID (assigned part set) and DRCPRM (scaling factor) on *CONTROL_SHELL [1].

In this study, we will first introduce the theoretical background of the constraint approach. Then, we will mainly demonstrate the necessity of this approach in implicit applications and the potential usefulness in explicit analyses.

2 The drilling rotation constraint method

The geometry of a shell finite element is defined by its thickness and a reference surface or mid-surface, which may be curved in space. Load is carried by a combination of membrane action and bending action. It exhibits 6 degrees of freedom at each node, 3 translations and 3 rotations.

The two rotations about in-plane axes are used to describe the bending and twisting stiffness of a shell element. The third rotational degree-of-freedom about the shell normal allows easy connection to other shell or beam elements. But it is not needed for shell kinematics itself, because in-plane deformations can be described just by interpolating the nodal displacements. However, no stiffness corresponding to the torsional rotation degree-of-freedom exists in those shell formulations. All the resistance to this rotation at each node comes directly from the coupling of the rotations of surrounding non-planar elements. That means for curved shell topologies, the drilling rotation is resisted by bending stiffness of adjacent elements. But for flat shell topologies, this special degree-of-freedom is totally free to spin. This zero stiffness leads to a singular stiffness matrix and therefore an unsolvable system of equations.

There are three different possibilities to prevent such singularities. First of all, kinematic constraints can be applied on these unconstrained degrees of freedom at global stiffness matrix level. This is the so-called *automatic single point constraint method (AUTOSPC)* which is also available in LS-DYNA. In this approach, the global stiffness matrix is examined for singular values depending on some given tolerance. Such a singularity is then constrained by setting the associated degree of freedom to zero [2]. Secondly, it would be possible to use a *local constraint method* where kinematic constraints are added on local element level. That means, depending on a local curvature criterion, single point constraints are added and/or deleted as deformation proceeds. Finally, rotational stiffness can be added in form of a fictitious torsional spring to penalize the drill rotation. This approach is the main topic of the present study. It is called the *drilling rotation constraint method (DRCM)* and will be described in more detail in the following.

The DRCM tries to avoid spurious energy modes associated with the drilling degree-of-freedom by adding a small amount of rotational stiffness. It has been shown that it is necessary not only to add stiffness contribution to the stiffness matrix but also to incorporate a corresponding force vector to achieve consistence.

The approach starts with the observation of kinematics on element level. As shown in Fig. 1, the following quantities are needed with respect to a specific node n : the rotational velocity $\boldsymbol{\omega}_n$ of this node, as well as coordinates \mathbf{x}_n , \mathbf{x}_{n-1} , \mathbf{x}_{n+1} and velocities \mathbf{v}_n , \mathbf{v}_{n-1} , \mathbf{v}_{n+1} of the node itself (n) and the two adjacent nodes ($n-1$ and $n+1$). With that information, a generalized drilling strain rate for node n can be defined as

$$\dot{\varepsilon}_n^{\text{drill}} = \boldsymbol{\omega}_n \cdot \mathbf{n}_n - \frac{(\mathbf{v}_{n+1} - \mathbf{v}_n) \cdot \mathbf{n}_n \times (\mathbf{x}_{n+1} - \mathbf{x}_n)}{2\|\mathbf{x}_{n+1} - \mathbf{x}_n\|^2} - \frac{(\mathbf{v}_{n-1} - \mathbf{v}_n) \cdot \mathbf{n}_n \times (\mathbf{x}_{n-1} - \mathbf{x}_n)}{2\|\mathbf{x}_{n-1} - \mathbf{x}_n\|^2}$$

where \mathbf{n}_n is the normal vector at node n . The subscripts indicate the node that the corresponding quantity is associated with.

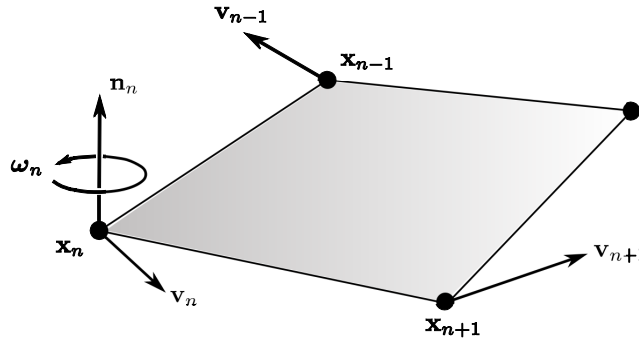


Figure 1: Illustration of kinematics for drilling constraint approach

This generalized drilling strain rate is converted into a generalized stress rate by associating a rotational stiffness to the drilling degree of freedom. Experiments together with hand-written calculations lead to the following expression for the generalized stress rate

$$\dot{\sigma}_n^{\text{drill}} = 0.0005 k E \dot{\varepsilon}_n^{\text{drill}}$$

where k is a user defined scaling parameter (DRCPRM), which is 1.0 by default. Here E is the Young's modulus for the shell element in question. The principle of virtual work results in an expression for the internal force in terms of the generalized stress and shell element geometry as

$$\mathbf{f}_n = V \sigma_n^{\text{drill}} \mathbf{B}_n^T$$

with V being the volume of the element and with the corresponding B-operator:

$$\mathbf{B}_n = \left[\mathbf{n}_n, \frac{\mathbf{n}_n \times (\mathbf{x}_{n+1} - \mathbf{x}_n)}{2\|\mathbf{x}_{n+1} - \mathbf{x}_n\|^2} + \frac{\mathbf{n}_n \times (\mathbf{x}_{n-1} - \mathbf{x}_n)}{2\|\mathbf{x}_{n-1} - \mathbf{x}_n\|^2}, -\frac{\mathbf{n}_n \times (\mathbf{x}_{n+1} - \mathbf{x}_n)}{2\|\mathbf{x}_{n+1} - \mathbf{x}_n\|^2}, -\frac{\mathbf{n}_n \times (\mathbf{x}_{n-1} - \mathbf{x}_n)}{2\|\mathbf{x}_{n-1} - \mathbf{x}_n\|^2} \right]$$

Finally, the stiffness matrix is given by

$$\mathbf{K}_n = 0.005 k E V \mathbf{B}_n^T \mathbf{B}_n$$

where the geometric contribution is neglected.

The choice for the user defined scaling factor DRCPRM will affect the solution in a way that very small values would lead to nearly singular stiffness and therefore poor convergence behavior in implicit analyses. On the other hand, high values for DRCPRM would add too much stiffness to the system, and therefore inaccurate results could be obtained. We will see in the examples that the default value of DRCPRM=1.0 seems to be a good compromise between the two extrema.

3 Numerical examples

3.1 Flat vs. curved geometry

A simple four-element test is used to demonstrate the dependence of drilling stiffness on the shell surface curvature. In the first case, a flat geometry is used and the middle node gets loaded with a torsional moment. The results of implicit and explicit analyses of this problem with activated and non-activated drilling rotation constraint lead to the expected results, see Figure 2. With the constraint, the elements rotate about the normal, but not without the additional stiffness. It should be emphasized that the drill constraint is the default behavior in implicit, but it is only optional in explicit analyses.

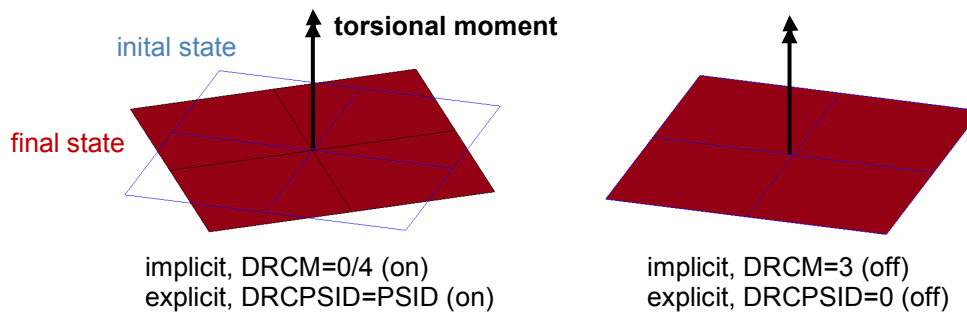


Figure 2: Flat shell geometry with torsional loading

If the initial coordinate of the middle node is altered in such a way that a curved surface is obtained, the variants with drill stiffness activated lead to nearly the same rotation as before. But without the drill stiffness a little rotation is obtained now because of the coupling to the bending rotations as shown in Figure 3 on the right.

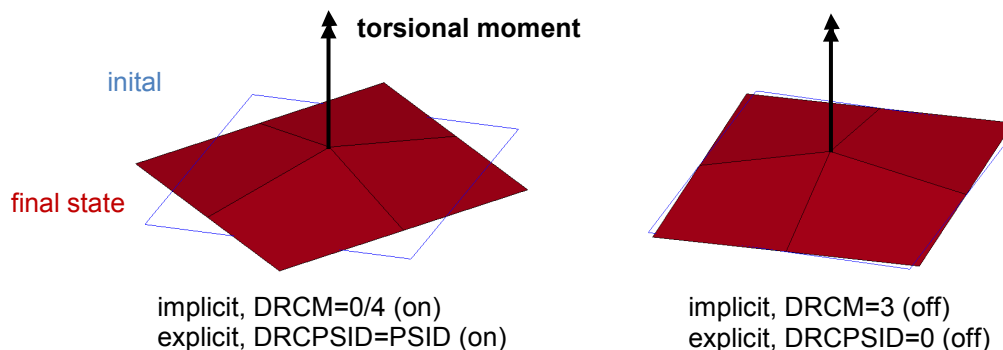


Figure 3: Curved shell geometry with torsional loading

3.2 Pre-twisted cantilever

A pre-twisted steel cantilever of dimensions 1 mm x 30 mm x 100 mm is modeled with quadrilateral shell elements and loaded at the tip end. Nonlinear static implicit analysis is chosen with a load increase from 0 to 10 N. An exemplary discretization is given in Figure 4. Convergence studies of the final displacement in loading direction are made with 6 different discretization levels: 12, 48, 120, 480, 1920, and 7680 elements. The corresponding edge lengths and warpage angles of the individual elements are 15 mm/20°, 7.5 mm/10°, 5 mm/6°, 2.5 mm/3°, 1.25 mm/1.5°, and 0.63 mm/0.8°, whereas the thickness is constantly 1 mm throughout the simulations. Elastic material is used with $E = 210$ GPa and $\nu = 0.3$.

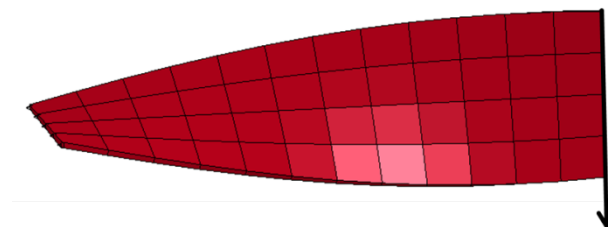


Figure 4: Pre-twisted cantilever with end load

First of all, shell elements without enhanced warping stiffness were tested, i.e. ELFORM=2 with BWC=0 and ELFORM=16 with IHQ=0. With the default drilling stiffness parameter DRCPRM=1.0 the resultant displacement converges to a value of 5 mm and good results are already obtained with the coarsest mesh (only 4 % error) as shown in Fig. 5 on the left. With substantially higher drilling stiffness, namely DRCPRM=100, convergence is also nice, but the results are slightly stiffer than before. On the other hand, a smaller drilling stiffness leads to a slowly converged solution of about 8mm, which is far too soft, i.e. the “missing” stiffness really impinges the solution.

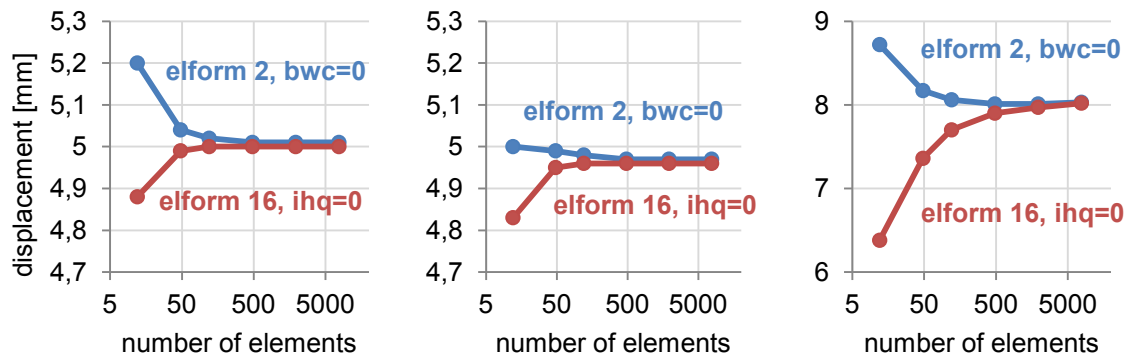


Figure 5: convergence study with DRCPRM = 1.0 (left), 100.0 (middle), and 0.01 (right)

The same study was done with enhanced warping stiffness for both element types, which means ELFORM=2 is used together with BWC=1 and ELFORM=16 comes with hourglass type IHQ=8. This does not have a big effect on the solution with DRCPRM=1.0 or DRCPRM=100.0. But the low drilling stiffness of 0.01 now gets rescued by the additional warping stiffness as shown in Fig. 6 on the right.

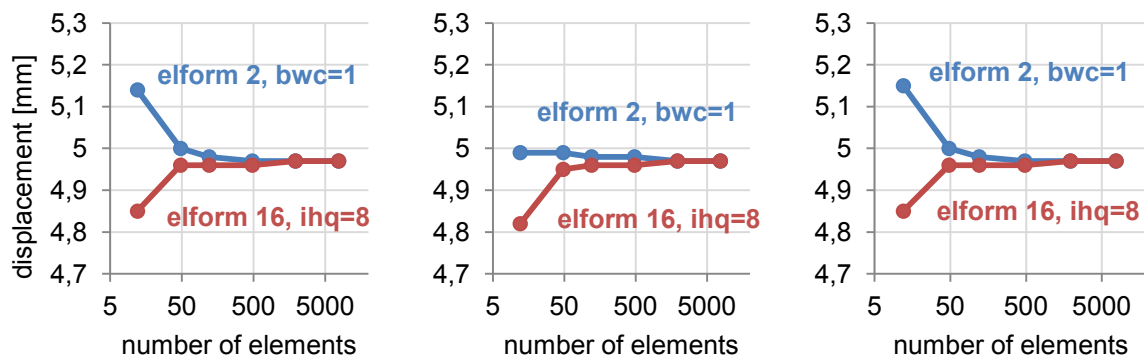


Figure 6: convergence study with DRCPRM = 1.0 (left), 100.0 (middle), and 0.01 (right)

3.3 Simplified crashrail

In the following example, a quarter model of a steel front rail is deformed in its axial direction. The input of this crash box test case can be found on www.dynaexamples.com. Three variants of static implicit simulations with different stiffness scaling factors are compared. Therefore DRCPRM on *CONTROL_IMPLICIT_SOLVER is set to 0.01 (a), 1.0 (b), and 100.0 (c).

The final deformed shape indicates no big difference between variants a and b (see Fig. 7). It seems that a reduction of the default factor does not improve the results. But variant c shows significantly different deformation behavior due to the higher stiffness and also the plastic strains (ranging from 0.0 to 0.6 in Fig. 7) are noticeably different. The same conclusions can be drawn from the resultant force evolution. A remarkably higher force level is obtained with variant c, whereas a and b do not differ much.

If the computational effort is compared and the default value of DRCPRM=1.0 (b) is used as a reference, it can be seen that a reduction of the stiffness (a) increases the numerical cost by a factor of 2 due to inferior convergence. On the other hand, an increase of the torsional stiffness (c) has no big effect on CPU time, it is about the same as for the default (b).

This parameter study shows that the default value of DRCPRM=1.0 seems to be a good choice to balance quality of results and computational effort.

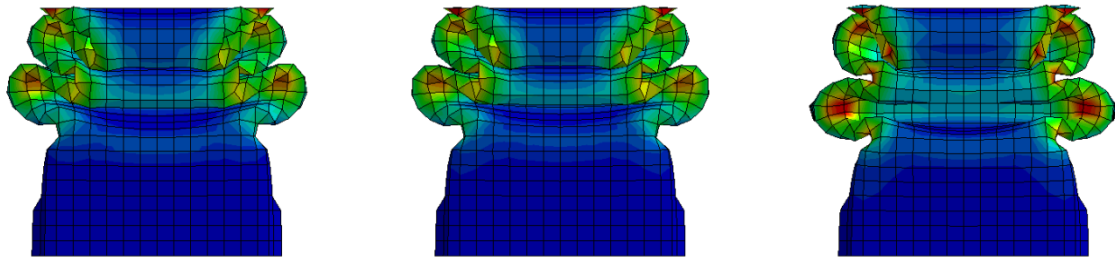


Figure 7: Deformed crashrail with DRCPRM=0.01 (left), 1.0 (middle), and 100.0 (right)

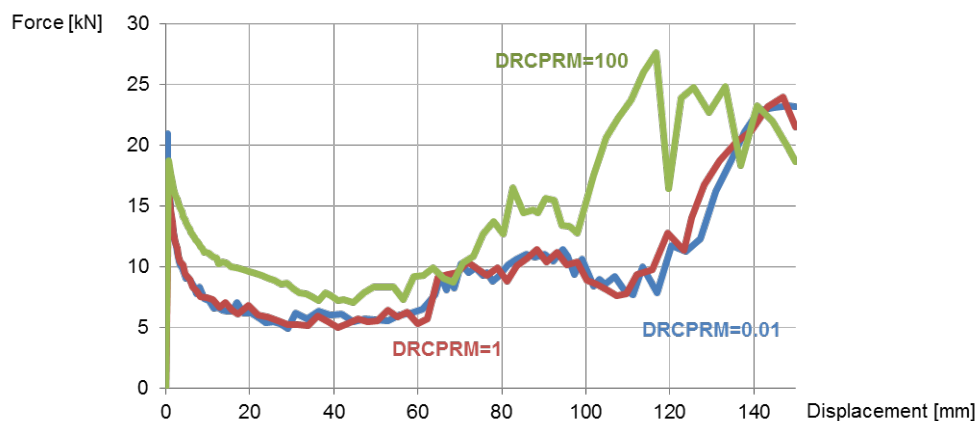


Figure 8: Load displacement curve of simplified crashrail with different drill rotation stiffnesses

The same study with the crash rail was done using explicit dynamic analysis (DRCPSID and DRCPRM are set on *CONTROL_SHELL then), where similar results are obtained when it comes to deformations or force levels. When it comes to the computational cost, it can be observed that the activation of the constraint method increases the CPU time by about 20% which is due to the additional calculations of the drilling constraint force as described in section 2. No real difference in terms of computational cost can be seen between the three variants though.

3.4 Channel forming

An explicit analysis of a channel forming process is examined, where a quarter model with appropriate symmetry conditions undergoes a deformation as can be seen in Fig. 9. The material is drawn over a 90 degree radius and it turns out that the free edge shows some “wavy” behavior when shell element type 2 and no drilling stiffness is used, which is the default setting in explicit. If the rotational constraint is activated via DRCPSID for the sheet, the free edge becomes straight as expected (Fig.9 on the right).

The reason seems to be that some regions of the structure are initially flat giving room to free spinning drill rotations, as illustrated in form of a vector plot in Fig. 10, where the nodal rotations are with respect to the vector direction (right hand rule), i.e. vectors pointing in the normal direction of a shell element indicate rotational spin. Without the constraint, a lot of such rotations can be observed in a non-smooth distribution, which seems to be responsible for the “wavy” edge effect. On the other hand, nodal rotations are more meaningful and smoothly distributed with the activated constraint and therefore the free boundary stays straight.

As already discussed in section 3.2, it also helps in this example to use enhanced warping stiffness to get improved behavior of the deformed geometry. But nonetheless, the nodal rotations can only get under control as shown in Fig. 10 with the drilling constraint activated.

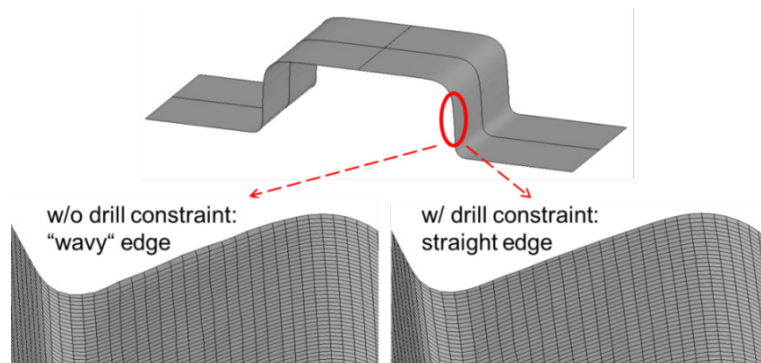


Figure 9: Deformation after channel forming process

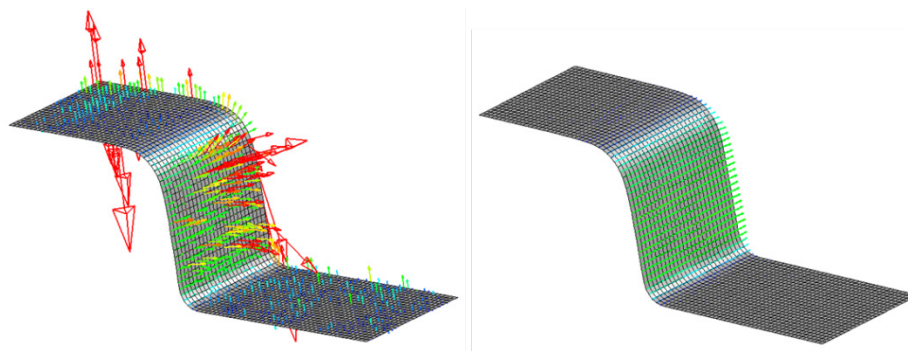


Figure 10: Vector plot of nodal rotations without (left) and with drill stiffness (right)

3.5 Spot weld connections

Punctual connections between metal parts, e.g. spot welds or rivets, are often discretized by single beam or solid elements fastened to shell element components. The deformation of such an assembled structure leads to local forces and moments acting on the shell elements at the connection point. The nodal rotations of individual nodes in these areas can become important in this context.

Often, point-wise connected areas of the structure are geometrically flat in the beginning (e.g. flanges of automotive parts), but they can get highly deformed, i.e. curved and warped, under crash load conditions. For the drilling degrees-of-freedom this means, that torsional rotations are free to spin in the early stages and they can notably be amplified by those local loads. In later stages with ongoing deformation, those rotations can affect the bending behavior around the spot weld, since rotations are coupled in curved geometries as already mentioned above. Usually, this fact does not seem to influence the overall solution. But sometimes, e.g. if unexpectedly large deformations and plastic strains can be seen in the vicinity of such a punctual connection, it could be helpful to activate the drilling constraint for the connected shell parts.

To demonstrate the effect of the drill stiffness method in a spot weld assembled structure, a T-bar component test with horizontal impact loading is used. Most differences can be seen when nodal rotations are plotted as vectors as shown in Fig. 11. The spectrum range for the rotations goes from 0 to $3.14 (\pi)$ which implies that the maximum is equal to a rotation of 180° . It can be seen that huge rotations take place without the constraint. As already mentioned this is not automatically a problem, because drill rotations do not have an effect in flat geometries. But it is not yet totally understood, what happens when those torsional rotations become coupled with the bending modes during the deformation process, i.e. when the surface becomes curved. At least in this example, the rotations are much smaller if the constraint is activated and local deformations around the spot welds are also decreased resulting in maximum plastic strain changing from 0.36 (w/o constraint) to 0.24 (w/ constraint).

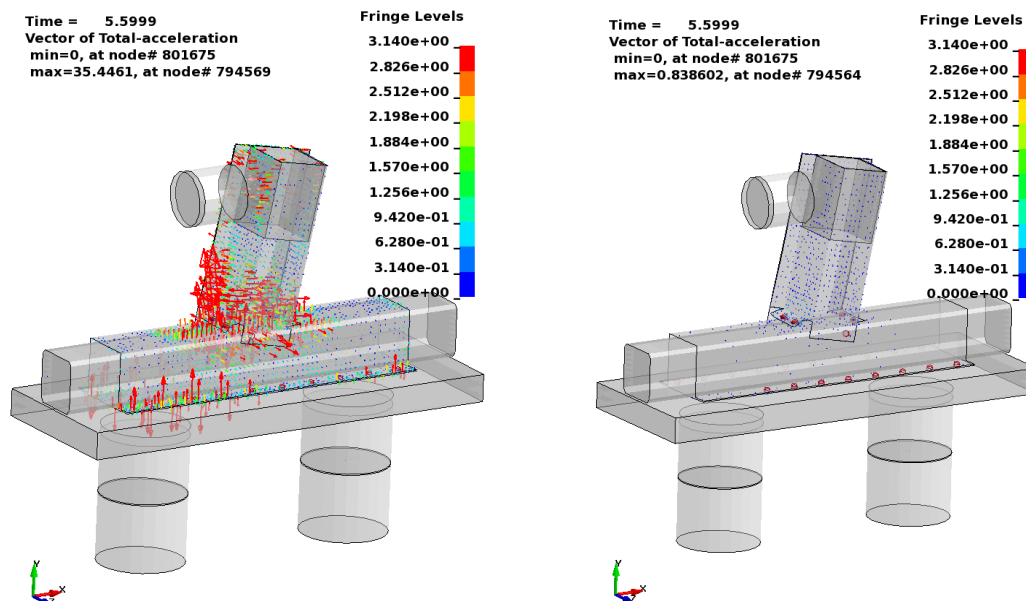


Figure 10: Vector plot of nodal rotations without (left) and with drill stiffness (right)

4 Summary

An attempt was made to provide more insight into the topic of shell element's drilling degree-of-freedom. The necessity of an appropriate constraint method in form of an additional torsional stiffness for implicit analyses is obvious. Therefore it is mandatory to be the default setting in LS-DYNA implicit calculations. This is not the case in explicit analyses, where this option has to be activated by the user. It was shown in several numerical tests, that it might be helpful in some situations to achieve more robust or even more accurate results. It has to be taken into account that the CPU cost can increase by up to 20% when this method is used in an explicit run. Therefore it makes sense to define it only for selected "critical" parts of the structure, where improvements are to be expected. The default value for the stiffness scaling factor seems to be a good choice in most cases. Nonetheless, one should bear in mind that this is a non-physical additional stiffness that might have an influence on the structural stiffness.

5 Literature

- [1] Hallquist, J. O.: Draft version of *LS-DYNA® Keyword User's Manual Volume I*, Livermore Software Technology Corporation, March 2013.
- [2] Hallquist, J. O.: *LS-DYNA® Theory Manual*, Livermore Software Technology Corporation, March 2006.